SVD-Aided UKF Adaptation for Nanosatellite Attitude Estimation under Uncertain Process Noise Conditions

Chingiz Hajiyev,[1] Demet Cilden-Guler[2]

[1]Istanbul Technical University, Faculty of Aeronautics and Astronautics, 34469, Istanbul, Turkey; email: cingiz@itu.edu.tr (Corresponding author)

[2]Istanbul Technical University, Faculty of Aeronautics and Astronautics, 34469, Istanbul, Turkey; email: cilden@itu.edu.tr

ABSTRACT:

In this work, the adaptation of the process noise covariance matrix for the non-traditional attitude filtering technique is discussed. The nontraditional attitude filtering technique integrates the Unscented Kalman Filter (UKF) and Singular Value Decomposition (SVD) approaches to estimate the attitude of a nanosatellite. It is shown in this study that the process noise bias and process noise increment type system changes will cause a change in the statistical characteristics of the innovation sequence of UKF. Influence of these type of changes to the innovation of UKF is investigated. For differences in between the process channels, the Q (process noise covariance) adaptation strategy with multiple scale factors is specifically recommended. We analyze the performance of the multiple scale factors-based adaptive SVD-Aided UKF (ASaUKF) in the cases of process noise increment and bias, which can be caused by variations in the satellite dynamics or space environment. The adaptive and non-adaptive variants of the non-traditional attitude filter are compared through simulations in order to estimate the attitude of a nanosatellite.

This is an Author Accepted Manuscript version.

AUTHOR KEYWORDS: attitude estimation, unscented Kalman filter, adaptive filtering, nanosatellite, process noise, magnetometer, Sun sensor

INTRODUCTION:

The observations in a standard attitude filter can be referenced to the Earth's magnetic field vector or any of the direction vectors to the Sun, star, or other celestial body. As a foundational approach to addressing the problem of attitude estimation with direction vector measurements, the Kalman filtering technique can be employed. This technique integrates the measurements in accordance with the satellite dynamics propagation model, facilitating a precise assessment of the satellite's orientation. In nonlinear measurements-based (traditional) approaches, the reference directions can directly be utilized to generate a Kalman filter for satellite attitude and rate estimates (Hajiyev and Cilden-Guler 2017; Soken and Hajiyev 2014; Springmann and Cutler 2014). In linear measurements-based (nontraditional) approaches, the observations are first handled in a single-frame method for establishing a linear set of measurements for the filtering stage, which might be Extended Kalman filter (EKF) (Hajiyev et al. 2016; Hajiyev and Bahar 2003; Hajiyev and Cilden-Guler 2017; Mimasu and Van der Ha 2009) or Unscented Kalman filter (UKF) (Cilden et al. 2017; Gui et al. 2023b; a; Soken and Sakai 2020). The nontraditional approach demonstrates the capability to maintain robustness even when there are changes in measurement noise covariance, leading to enhanced accuracy performance (Cilden-Guler et al. 2017b). The article (Xue et al. 2023) presents an adaptive filter system based on the multistate constraint Kalman filter in position, orientation and measurement noise covariance factor estimation, where it is then used in the filtering for adaptation without considering an uncertain process noise in the system.

Adjusting the process noise covariance of the filter presents a challenge for non-traditional attitude filters, as observed in previous studies. Changes in the disturbance torques, such as residual magnetic torque, inaccuracies in satellite dynamics modeling, or issues with actuators, lead to variations in the process noise covariance of the filter. Although the non-traditional attitude filter exhibits robustness against measurement variations, it lacks the ability to adapt to fluctuations in this specific type of process noise covariance e.g. change in the mass moment of inertia of the spacecraft or space environment. The process noise adaptation needs to be considered at this stage in order to have this ability on top of the robustness against measurement noise challenges. The study in (Almagbile et al. 2023) stated that a traditional Kalman filter is typically utilized when the covariance matrices are known and constant. However, when the covariance matrices are unknown and time-varying, various adaptive estimation procedures must be developed to estimate their statistical information. An adaptive fading UKF algorithm based on the correction of process noise covariance (Q-adaptation) for the case of mismatches with the model is proposed in (Soken and Hajiyev 2011). The Sage-Husa adaptive Kalman filter and innovation-based adaptive Kalman filter approaches are employed in (Almagbile et al. 2023) for adapting the measurement covariance matrix. In order to improve the performance of data fusion under abnormal measurement noise, it is proposed to use an adaptive M-estimation robust unscented Kalman filter in (Sun et al. 2023). They combine Huber's linear regression problem with the covariance matching approach to produce the adaptive matrix, which uses the innovation covariance estimator based on fading memory index weights to change the measurement noise covariance adaptively. Another study of (Qiu et al. 2020) presents an adaptive resilient spacecraft attitude estimate algorithm based on Huber and covariance matching. The measurement noise is calculated using robust filtering by building a nonlinear regression model whereas the process noise is reduced by incorporating a fading component.

The paper of (Li et al. 2016) presents a robust UKF extension which provides trustworthy state estimations in the presence of unknown process noise and measurement noise covariance matrices. To increase dynamic state estimation accuracy, another research provides an adaptive filtering strategy based on innovation and residual to adaptively estimate Q and R of EKF (Akhlaghi et al. 2018). A variational

Bayesian-based adaptive Kalman filter for linear Gaussian state-space model with inaccurate process and measurement noise covariance matrices is proposed in (Huang et al. 2018). The state, as well as the expected error and measurement noise covariance matrices, are inferred using the variational Bayesian technique using inverse Wishart priors. Another study on slide window variational adaptive Kalman filter is presented in (Huang et al. 2020) in case of inaccurate state and measurement noise covariance matrices. The algorithms are designed based on the forward Kalman filtering, the backward Kalman smoothing, and the online estimates of noise covariance matrices. Similarly, in (Huang et al. 2021), variational adaptive Kalman filter with Gaussian-inverse-Wishart mixture distribution is implemented for partially unknown state and measurement noise covariance matrices. The system state vector together with the process noise covariance matrix and the measurement noise covariance matrix are jointly estimated. In (Zhu et al. 2023), the coefficient of the process noise covariance matrix is estimated based on the variational Bayesian method and improved by the sample screening technique by dimension. The study of (Kim et al. 2021) introduces an augmented adaptive unscented Kalman filter to estimate both the diagonal process noise covariance matrix and the unknown inputs. A selective scaling method is introduced in that study to improve the convergence property of the filter. A method is presented in (Iezzi et al. 2023) for localization that employs an adaptive Extended Kalman Filter exploiting statistical techniques to overcome the inaccuracies of conventional EKF when the noise of the environment or of the instrumentation is time-varying or unknown. Another study of (Xi et al. 2018) proposes an adaptive process noise covariance Kalman filter that updates the process noise covariance matrix of the KF by maximizing the evidence density function. A robust filtering method combined multi-factor scaling and bias estimation is proposed in (Xu et al. 2022) based on the estimation of variances. An optimal information fusion methodology based on adaptive and robust UKF is presented in (Wang et al. 2021) for multi-sensor nonlinear stochastic systems. Their simulation findings show that the proposed strategy works well in the presence of time-varying process error and measurement noise covariance.

In (Hajiyev and Cilden-Guler 2023), it is demonstrated how to change the process and measurement noise covariance matrices at the same time for a nontraditional attitude filtering technique. The authors' study like the other studies mentioned in this section only considers the event of uncertain process noise caused by changes in the environment or satellite dynamics. It is shown in this study; however, that both of the process noise bias and process noise increment type system changes will cause a change in the statistical characteristics of the innovation sequence of UKF. The theoretical basics of the Q-adaptive SVD-aided UKF with uncertain process noise mean and covariance are developed and presented. For the purpose of estimating a nanosatellite's attitude, simulations are compared using the adaptive and non-adaptive versions of the nontraditional attitude filter in the presence of process noise bias and process noise increment type system changes.

In the following sections, we first describe the rotational motion of the satellite and the measurement models for the attitude sensors. The attitude estimation algorithms are then given with the influence of process noise changes to the innovation. The theoretical basics of the Q-adaptive SVD-aided UKF with uncertain process noise mean and covariance are presented. Analyses and findings are provided after providing specifics of the proposed estimation filter with multiple factor adaption characteristics. Finally, in the concluding section of the work, a summary and conclusion are provided.

SATELLITE ROTATIONAL MOTION AND ATTITUDE MEASUREMENT MODELS:

The satellite's kinematics equation of motion may be written using the quaternion attitude representation as,

$$\dot{\boldsymbol{q}}(t) = \frac{1}{2}\Omega(\boldsymbol{\omega}_{BR}(t))\boldsymbol{q}(t) \ . \qquad (1)$$

Here $\boldsymbol{q}$ comprises of four attitude parameters in the quaternion, $\boldsymbol{q}=\begin{bmatrix} q_1 & q_2 & q_3 & q_4 \end{bmatrix}^T$ where it satisfies the condition that the norm of the elements is 1. We can recast the quaternion because the last term is a scalar and the first three terms are vector terms as $\boldsymbol{q}=\begin{bmatrix} \boldsymbol{g}^T & q_4 \end{bmatrix}^T$, $\boldsymbol{g}=\begin{bmatrix} q_1 & q_2 & q_3 \end{bmatrix}^T$, $\Omega(\boldsymbol{\omega}_{BR})$ is 4×4 skew symmetric matrix composed by the components of $\boldsymbol{\omega}_{BR}=\begin{bmatrix} \omega_1 & \omega_2 & \omega_3 \end{bmatrix}^T$ that is the angular velocity vector of body frame with respect to the reference (orbital) frame.

It is essential to describe the angular rate vector of the body in regard to the inertial axis frame separately from the angular velocity vector, $\boldsymbol{\omega}_{BI}=\begin{bmatrix} \omega_x & \omega_y & \omega_z \end{bmatrix}^T$. $\boldsymbol{\omega}_{BI}$ and $\boldsymbol{\omega}_{BR}$ can be related via,

$$\boldsymbol{\omega}_{BR}=\boldsymbol{\omega}_{BI}-\mathbf{A}\begin{bmatrix} 0 & -\omega_o & 0 \end{bmatrix}^T. \tag{2}$$

Here, ω_o indicates the satellite's angular orbital velocity. In (3), $\mathbf{A}$ is the attitude matrix and the quaternions are linked to it by,

$$\mathbf{A}=(q_4^2-\left|\boldsymbol{g}\right|^2)I_{3\times 3}+2\boldsymbol{g}\boldsymbol{g}^T-2q_4\left[\boldsymbol{g}\times\right]. \tag{3}$$

I_{3x3} is the identity matrix with the dimension of 3×3 and $\left[\boldsymbol{g}\times\right]$ is the skew-symmetric matrix whose elements are the components of $\boldsymbol{g}$ vector.

Based on Euler's equations, it is possible to deduce the satellite's dynamic equations,

$$J\frac{\boldsymbol{\omega}_{BI}}{dt}=\boldsymbol{N}_d-\boldsymbol{\omega}_{BI}\times\left(J\boldsymbol{\omega}_{BI}\right), \tag{4}$$

where J is the principal moments of inertia matrix as $J=diag\left(J_x,J_y,J_z\right)$ and $\boldsymbol{N}_d$ is the vector of disturbance torque affecting the nanosatellite.

This study outlines our approach for attitude determination on a nanosatellite that incorporates both magnetometers and a Sun sensor as attitude sensors. To determine the attitude, it is necessary to establish the unit vectors in the reference orbit frame that correspond to the unit vectors measured by the sensors in the spacecraft body frame. The measurement models presented in this study depict the relationships between these computed and measured unit vectors, facilitating accurate attitude determination. The magnetometer measurement model is as follows,

$$\boldsymbol{B}_b = \mathbf{A}\boldsymbol{B}_o + \boldsymbol{\xi}_1 \tag{5}$$

Here $\boldsymbol{B}_b$ is the magnetic field vector measured in the body frame, $\boldsymbol{B}_o$ is the orbit frame's computed magnetic field vector and $\boldsymbol{\xi}_1$ is the zero-mean Gaussian white noise.

In orbit frame, the Sun direction measurement model can be written as follows,

$$\boldsymbol{S}_b = \mathbf{A}\boldsymbol{S}_o + \boldsymbol{\xi}_2 \tag{6}$$

Here $\boldsymbol{S}_b$ is the Sun direction vector as measured in the body frame, $\boldsymbol{S}_o$ is the orbit frame's determined Sun direction vector and $\boldsymbol{\xi}_2$ is the zero-mean Gaussian white noise. It is assumed that that the magnetometers and Sun sensors are calibrated against any bias and/or misalignment.

INTEGRATION OF SVD AND UKF FOR ATTITUDE ESTIMATION:

The nontraditional attitude estimation procedure that is composed of two stages as singular value decomposition (SVD) and unscented Kalman filter (UKF) is presented in this section. The algorithm of Singular Value Decomposition Aided Unscented Kalman Filter (SVD-aided UKF) is named SaUKF for short throughout the text.

Single-frame attitude estimate techniques encompass methods such as SVD, q-method, QUEST, FOAM, and others (Markley and Mortari 2000). All these techniques aim to minimize the loss function as defined by Wahba (1965). In this instance, the SVD approach is selected for its superior robustness (Cilden-Guler et al. 2017a; Vinther et al. 2011).

Given a set of $n \geq 2$ vector measurements, $\hat{\mathbf{u}}_B^i$, in the body system, choosing to minimize the loss function given as for an ideal attitude matrix, A, is one possibility,

$$J(\mathbf{A}) = \sum_{i=1}^{n} w_i \left| \hat{\mathbf{u}}_B^i - \mathbf{A}\hat{\mathbf{u}}_R^i \right|^2 \tag{7}$$

where w_i is the weight of the ith vector measurement, $\hat{\mathbf{u}}_R^i$ is the vector in the reference frame. This optimization problem can be solved using the SVD method. An attitude determination algorithm based on SVD is provided in (Markley and Mortari 2000). SVD method also provides covariance matrix comprising the singular values (for details, please see (Markley and Mortari 2000)) . The filter achieves robustness against measurement faults through this initial pre-processing stage of SVD method that accurately determines the initial states, eliminating the need for arbitrary values but also gain the filter a reconfigurability capability for various sensor sets for different mission operation scenarios.

The UKF is based on the unscented transform, a deterministic sampling approach used to get a reduced set of sample points (or sigma points) from the states' previous mean and covariance. These sigma points are nonlinearly processed, and the modified sigma points are used to calculate the posterior mean and covariance (Julier et al. 2000).

Because the UKF is formed using discrete-time nonlinear equations, the process model is represented by the equations below,

$$\mathbf{x}(k+1) = \mathbf{f}(\mathbf{x}(k), k) + \mathbf{w}(k), \tag{8}$$

$$\mathbf{y}(k) = \mathbf{H}\mathbf{x}(k) + \boldsymbol{\xi}(k). \tag{9}$$

Here, $\mathbf{x}(k)=\left[\boldsymbol{q}(k)^T \quad \boldsymbol{\omega}_{BI}(k)^T\right]^T$ is the 7x1 state vector. As all the states are measured, $\mathbf{y}(k)$ is the 7x1 measurement vector, which is composed of the quaternion measurements determined by the SVD method and the angular velocities by the rate gyros. Moreover $\mathbf{w}(k)$ and $\boldsymbol{\xi}(k)$ are the process and measurement error noises, which, according to the assumption, are processes with Gaussian white noise with zero mean and a covariance of $\mathbf{Q}(k)$ and $\mathbf{R}(k)$ respectively, $\mathbf{H}$ is the measurement matrix of system.

The detailed explanation of the well-known Unscented Kalman Filter (UKF) procedure for the process specified in equations (8) and (9) can be found in (Hajiyev et al. 2019). However, to maintain brevity, the step-by-step procedure is not provided in this paper.

INFLUENCE OF PROCESS NOISE CHANGES TO THE INNOVATION OF UKF:

The statistical properties of UKF's innovation will be changed due to process noise bias and process noise increment type system changes. The impact of such types of changes on UKF innovation is examined in this section.

Influence of Process Noise Increment to the Innovation:

Let the UKF process the measurements and a process noise increment occurs at the iterations $k \geq \tau$. Process noise increment can be simulated by multiplying the process noise vector by the diagonal matrix $\mathbf{\Phi}(k)$, the diagonal elements of which satisfy the following condition: $\sigma_{ii}(k) \geq 1$, $(i=\overline{1,s})$ for $\forall\ k \geq \tau$ (s is the dimension of the process noise vector). The diagonal elements of matrix $\mathbf{\Phi}(k)$ can be represented as follows:

$$\sigma_{ii} = \begin{cases} 1: \text{ there is no change in system noise} \\ >1: \text{changes in system noise} \end{cases}$$

The mathematical model of process in this case can be written in the form:

$$\mathbf{x}(k+1) = \mathbf{f}(\mathbf{x}(k), k) + \mathbf{\Phi}(k)\mathbf{w}(k) , \tag{10}$$

The following theorem was proven in (Hajiyev and Cilden-Guler 2023).

Theorem 1: If the UKF process the measurements and a process noise increment occurs at the iteration step $k = \tau$. Then at the all $k \geq \tau$ steps the process noise increment leads to increment in the innovation covariance.

Theorem 1 shows that process noise increment type system changes will lead to an increment in UKF's innovation covariance.

Influence of Process Noise Bias to the Innovation:

Assumption. In this section, the process noise is assumed to be biased and can be represented as a of sum of random $w(k)$ and constant $\delta(k)$ components.

The process and measurement model equations in this case can be written as,

$$\mathbf{x}_b(k+1) = \mathbf{f}(\mathbf{x}(k), k) + \boldsymbol{\delta}(k) + \mathbf{w}(k) , \tag{11}$$

$$\begin{aligned} \mathbf{y}_b(k) &= \mathbf{H}\mathbf{x}_b(k) + \boldsymbol{\xi}(k) \\ &= \mathbf{H}\left[\mathbf{f}(\mathbf{x}(k-1), k-1) + \boldsymbol{\delta}(k-1) + \mathbf{w}(k-1)\right] + \boldsymbol{\xi}(k) \\ &= \mathbf{H}\left[\mathbf{f}(\mathbf{x}(k-1), k-1) + \mathbf{w}(k-1)\right] + \mathbf{H}\boldsymbol{\delta}(k-1) + \boldsymbol{\xi}(k) \\ &= \mathbf{H}\mathbf{x}(k) + \mathbf{H}\boldsymbol{\delta}(k-1) + \boldsymbol{\xi}(k) = \mathbf{y}(k) + \mathbf{H}\boldsymbol{\delta}(k-1) \end{aligned} \tag{12}$$

Here, b in the index shows that the value is biased. It is clear that in this case the system state estimates will be biased.

Theorem 2: If the UKF process the measurements and a process noise bias occurs at the iteration step $k = \tau$, then at the all $k > \tau$ steps the estimation and innovation of UKF are biased and innovation bias is equal to the observed difference between the process bias and prediction bias.

Proof. See Appendix A.

A sampling covariance matrix of innovation is presented as statistics for detecting and compensating for changes in process noise. The innovation's sample covariance matrix can be written as: (Hajiyev et al. 2019):

$$\hat{\mathbf{S}}_{\nu}(k) = \frac{1}{M}\sum_{j=k-M+1}^{k} \mathbf{v}(j)\mathbf{v}^{T}(j) \tag{13}$$

where M is the width of the “sliding window”.

If there is a bias in the mean of the innovation at time τ, and the biased innovation is indicated by $\mathbf{v}_b(k)$, then the biased innovation is defined as,

$$\mathbf{v}_b(k) = \mathbf{v}(k)\ , \qquad k=1,2,\dots\ \tau-1 \tag{14}$$

$$\mathbf{v}_b(k) = \mathbf{v}(k) + \boldsymbol{\mu}(k), \qquad k=\tau,\tau+1,.. \tag{15}$$

where $\boldsymbol{\mu}(k)$ is an unknown innovation bias vector.

When k<τ, the following formula provides the mathematical expectation of the sample innovation covariance matrix (17)

$$E\left[\hat{\mathbf{S}}_{\nu}(k)\right] = \mathbf{P}_{\nu\nu}(k/k-1) = \mathbf{HP}(k/k-1)\mathbf{H}^{T} + \mathbf{R}(k) \tag{16}$$

Here $\mathbf{P}(k/k-1)$ is the extrapolation error covariance matrix. In the case of k$\geq\tau$, in the sample innovation covariance a biased innovation $\mathbf{v}_b(k) = \mathbf{v}(k) + \boldsymbol{\mu}(k)$ is used instead of an unbiased innovation $\mathbf{v}(k)$ [21].

$$\hat{\mathbf{S}}_{\nu b}(k) = \frac{1}{M}\sum_{j=k-M+1}^{k} \mathbf{v}_b(j)\mathbf{v}_b^{T}(j) \tag{17}$$

Remark 1. Note that the mean of innovation $\mathbf{v}_b(k)$ in this case is not zero, so formula (17) is not a sample covariance. In a “sliding window”, this is the mean square of innovation (MSI).

Statement. The bias in innovation leads to an increase in the mathematical expectation of the mean square of innovation.

Proof. The mathematical expectation of mean square of innovation (17) can be written as

$$E\left[\hat{\mathbf{S}}_{\nu b}(k)\right]=\frac{1}{M}E\left(\sum_{j=k-M+1}^{k}\left[\mathbf{v}(j)+\boldsymbol{\mu}(j)\right]\left[\mathbf{v}(j)+\boldsymbol{\mu}(j)\right]^T\right)=\frac{1}{M}\times$$
$$E\left(\sum_{j=k-M+1}^{k}\left[\mathbf{v}(j)\mathbf{v}^T(j)+\mathbf{v}(j)\boldsymbol{\mu}^T(j)+\boldsymbol{\mu}(j)\mathbf{v}^T(j)+\boldsymbol{\mu}(j)\boldsymbol{\mu}^T(j)\right]\right) \quad (18)$$

Taking into account $E\left[\mathbf{v}(k)\right]=0$, and the absence of correlation between the parameters $\mathbf{v}(j)$ and $\boldsymbol{\mu}(j)$, we have

$$E\left[\hat{\mathbf{S}}_{\nu b}(k)\right]=E\left[\hat{\mathbf{S}}_{\nu}(k)\right]+\frac{1}{M}E\left(\sum_{j=k-M+1}^{k}\boldsymbol{\mu}(j)\boldsymbol{\mu}^T(j)\right) \quad (19)$$

Comparison of expressions (18) and (19) proves the Statement. Consequently, the process noise bias will increase the mathematical expectation of the mean square of innovation.

It can be seen from the Theorem 2 and the Statement above that the process noise bias is transferred to the innovation bias and changes the mean square of innovation (17). The innovation bias $\boldsymbol{\mu}(k)$ leads to a change in the values of $\mathbf{v}_b(k)$ and the elements of the mean square of innovation. As a result, the bias in the process noise is transferred to the MSI. Thus, the MSI can be chosen as a monitoring statistic in the problem of compensating for changes in process noise.

Q-ADAPTIVE INTEGRATED SVD/UKF ATTITUDE ESTIMATION ALGORITHM:

In the integrated filtering procedure, one of the single-frame methods -SVD in our case- runs for providing the attitude and corresponding covariances. The Kalman-type filter -UKF in our case- is then processed with these estimated attitude terms as input. 'SaUKF' is used instead of 'SVD-aided UKF' and 'ASaUKF' instead of 'Q-Adaptive SVD-aided UKF' for short. In addition to the estimated quaternions, the estimation covariance obtained from the SVD is incorporated into the UKF method. It is utilized as the measurement noise covariance matrix for the filter, i.e. $R(k+1)=P_{svd}(k+1)$. As a result, this filtering approach is inherently resistant to measurement noise increments in particular. In the presence of a measurement error, the SVD's estimation covariance, which is also the filter's measurement noise covariance, rises, allowing the filter to run without being adversely damaged.

One problem for the attitude filters is adjusting the filter's process noise covariance matrix. It is critical to improve the process noise covariance as the environment changes. Any conditional modification that might affect the filter's process model is mentioned here. These include changes to the inertia parameters (for example, deployment or retraction of solar arrays, motion of robotic arms), changes to the disturbance torques (for example, when the satellite enters or escapes an eclipse), and changes to the controller parameters (for example, a failure), though a controller is not addressed in this study. While the measurement covariance is adapted automatically by the aid of SVD method, an external rule is employed to concurrently adjust the process covariance, ensuring that both covariances are adapted.

The noise increment type process noise change influences UKF's innovation covariance (Hajiyev and Cilden-Guler 2023). As a result, in the process noise covariance matching problem, the innovation covariance can be used as the monitoring statistic. The innovation covariance at the iteration steps $k \geq \tau$ can be written as,

$$\mathbf{P}_{vv}\left(k+1|k\right)=\mathbf{H}\left[\mathbf{P}^{*}\left(k+1|k\right)+\left[\mathbf{\Phi}(k)\right]^{2}\mathbf{Q}(k)\right]\mathbf{H}^{T}+\mathbf{R}(k+1) \tag{20}$$

Here $\mathbf{P}^*\left(k+1|k\right)$ is the extrapolation error covariance matrix without taking into account process noise.

Substituting the adaptive scaling matrix $\mathbf{\Lambda}(k)=\left[\mathbf{\Phi}(k)\right]^2$ into formula (20), after mathematical transformations we have

$$\mathbf{H\Lambda}(k)\mathbf{Q}(k)\mathbf{H}^T=\mathbf{P}_{vv}\left(k+1|k\right)-\mathbf{HP}^*(k+1/k)\mathbf{H}^T-\mathbf{R}(k+1) \tag{21}$$

After multiplying the expression (21) by $\mathbf{H}^T$ on the left and $\mathbf{H}$ on the right, we get

$$\mathbf{H}^T\mathbf{H\Lambda}(k)\mathbf{Q}(k)\mathbf{H}^T\mathbf{H}=\mathbf{H}^T\left[\mathbf{P}_{vv}\left(k+1|k\right)-\mathbf{HP}^*(k+1/k)\mathbf{H}^T-\mathbf{R}(k+1)\right]\mathbf{H} \tag{22}$$

The scaling matrix $\mathbf{\Lambda}(k)$ is defined from the formula (22) as

$$\mathbf{\Lambda}(k)=\left[\mathbf{H}^T\mathbf{H}\right]^{-1}\mathbf{H}^T\times\left[\frac{1}{M}\sum_{j=k-M+1}^{k}\mathbf{v}\left(j+1\right)\mathbf{v}^T\left(j+1\right)-\mathbf{HP}^*(k+1/k)\mathbf{H}^T-\mathbf{R}(k+1)\right]\times\mathbf{H}\left[\mathbf{Q}(k)\mathbf{H}^T\mathbf{H}\right]^{-1} \tag{23}$$

where its components compose the adaptive factors. The pseudocode for the proposed algorithm is given in the Table I.

Remark 2. Formula for the scaling matrix (23) can be used in two practical cases:

It can be used to adapt the real process noise covariance to the changing environment. If the real process noise increase, according to Theorem 1, the process noise increment leads to increment in the innovation and the innovation covariance. As seen from (23), in this case, the elements of the scaling matrix will increase and become more than 1. The simulations of Section VI.B are run for this case.

It can be used for verification of the process noise covariance. If the covariance matrix, Q used in the mathematical model of the system is larger than the real process noise covariance, as seen from (23), the denominator will increase and the scaling matrix will decrease. In this case, the elements of the scaling matrix will become less than 1. The simulations of Section VI.A are run for this case.

ANALYSIS OF SIMULATION RESULTS:

The research considers a tumbling satellite to evaluate the suggested techniques under critical measurement and environmental concerns. The principal moment of inertia is $J = \text{diag}\begin{bmatrix}0.055 & 0.055 & 0.017\end{bmatrix}$ kg m^2. The program runs for nearly one orbital cycle with the filter and sensors sampling at 1 Hz. Magnetometers and Sun sensors are chosen as the attitude sensors with the standard deviations of $\sigma_B = 300$ nT and $\sigma_S = 0.002$, respectively. The process noise covariance is set as $\mathbf{Q} = diag\begin{bmatrix}10^{-4}\mathbf{I}_{3\times3} & 10^{-9}\mathbf{I}_{3\times3}\end{bmatrix}$ for an initial matrix. The single-frame attitude estimation methods can be employed only when at least two measurements are available at the same time and the vectors are not parallel to one another. As a result, the single-frame approach is unsuccessful when the satellite is in shadow and two vectors are parallel. An eclipse period is inserted between the 500th and 1500th seconds to illustrate how the filter performs when used with a single-frame technique in these intervals. The first segment assesses the ASaUKF for process noise increments between 4500th and 5500th seconds. In the same interval, the second portion examines the adaptation for process noise bias.

Process Noise Increment Case:

We reveal that the nontraditional attitude filter may be R and Q adaptive at the same time. Similarly to the preceding part, the eclipse time ranges from 500th to 1500th seconds. As the process noise increases as, $\mathbf{Q} = \begin{bmatrix}10^{-4}\,\text{diag}(\eta_{1x3}) & 0_{3x3} \\ 0_{3x3} & 10^{-9}\,\text{diag}(\eta_{1x3})\end{bmatrix}$ between 4500th and 5500th s to test the efficacy of the suggested Q-adaptation method for the attitude filter by using the constant increment vectors of $\eta_{\text{low}} = \{10^2 \quad 2\times10^2 \quad 2\times10^3\}$; $\eta_{\text{medium}} = \{10^3 \quad 2\times10^3 \quad 2\times10^4\}$; $\eta_{\text{high}} = \{10^4 \quad 2\times10^4 \quad 2\times10^4\}$ for each channel of attitude and angular rates. Because we employ multiple measurement noise scaling factors, also known as adaptive factors, changing increments on each channel will result in distinct factors for each channel of the factor.

ASaUKF quaternion estimate errors are seen in Fig. 1. The Figure shows the case of having high process noise increments. The graphic shows three periods that are not as correctly assessed as the rest of the time. The first is the eclipse period, which lasts between 500 and 1500 seconds. Switching to a magnetometer-based estimate filter makes it easy to customize this interval. The second interval of having parallel vectors of sun and magnetic field directions about 3400th second is the same. The noisy interval is the third interval of process covariance between 4500 and 5500 seconds. We'd like to take a closer look at this time period. Table II shows the RMS errors for this interval for each filter and scenario. When closely examining the estimation error norms, it becomes apparent that the ASaUKF performance is not significantly affected by increasing noise increments from low to high levels, unlike the SaUKF.

In terms of process noise covariance, SaUKF calculations lack an adaptive framework. As a result, the estimate errors for SaUKF rise from low to high increment situations, but the estimation errors for ASaUKF do not vary substantially. This is an obvious result of each channel's effective adaptation in process covariance. This adaptation is carried out utilizing the adaptation factor shown in Fig. 2 for the situation of high process noise escalation. As a result, we may conclude that ASaUKF is more dependable than SaUKF for each process noise increment, even when attitude estimates continue to deteriorate. Figure 3 depicts various process noise increments for a better understanding of Table II. The increment values (η) are given the same for every channel as $\mathbf{Q} = \eta diag\left[10^{-4}\mathbf{I}_{3x3} \quad 10^{-9}\mathbf{I}_{3x3} \right]$.

As seen in this section, the increment is issued between 4500 and 5500 seconds intervals. RMS errors are estimated for each instance throughout this time period. The estimation error trend for each filter is plainly visible. It can be shown that the SaUKF has a rapid rise in estimating errors for this type of uncertainty produced by environmental changes. ASaUKF, on the other hand, grows considerably by the provided increment. The ASaUKF is unaffected by process noise increments, particularly in the beginning, and remains at the same error level, whereas the SaUKF has a jump in that interval and gradually grows subsequently.

Process Noise Bias Case:

To investigate the filter's ability to adapt to process bias faults, the algorithm is tested on three different types of faults: low, medium and high noise bias over a short period of time. Process noise biases are identified by adding the constant bias term to the process noise between 4500th and 5500th s.

For the test case the constant term is selected as $\delta = \{\delta_{\text{low}} \quad \delta_{\text{medium}} \quad \delta_{\text{high}}\}$ to represent low, medium, and high bias cases:

$$\delta_{\text{low}} = \begin{bmatrix} 0.005 & 0.005 & 0.005 & 0 & 0 & 0 \end{bmatrix}^T$$

$$\delta_{\text{medium}} = \begin{bmatrix} 0.008 & 0.008 & 0.008 & 0 & 0 & 0 \end{bmatrix}^T \; \delta_{\text{high}} = \begin{bmatrix} 0.012 & 0.012 & 0.012 & 0 & 0 & 0 \end{bmatrix}^T$$

The Root Mean Squares Errors (RMS) for SaUKF and ASaUKF for process noise bias cases are shown in Table III. The estimation errors from low to high levels of process noise bias show increase of error. In Fig. 4, quaternion estimations of ASaUKF algorithm are given, when having noise biases of δ_{high} level. As seen, using adaptive algorithm, the attitude quaternions can be estimated reasonably well for three out of four components, and overall quaternion estimation error norms. Adaptive factors for each channel of ASaUKF algorithm under process noise bias applied as δ_{high} are presented in Figure 5. The obtained results show that the bias type process noise changes can be compensated using the covariance scaling techniques.

CONCLUSIONS:

In this paper, the adaptive SVD-Aided UKF is proposed to estimate a nanosatellite's attitude an attitude filtering technique is proposed that adapts the process noise uncertainties. The bias and noise increment type process noise uncertainties are considered.

In this study it is proved that the process noise bias and process noise increment type system changes will cause a change in the statistical characteristics of the innovation sequence of UKF. Influence of these type of changes to the innovation of UKF is investigated. For differences between process channels, the adaptation strategy with multiple scale factors is specifically recommended. The proposed multiple scale factors-based adaptive SVD-Aided UKF's performance is investigated. It is proved in the manuscript that the bias type process noise change may be converted to the mean square of innovation of UKF and such type of changes can be compensated using the covariance scaling techniques.

Various levels of process noise bias and process noise increment type system changes are tested. Simulations are compared using the adaptive and non-adaptive versions of the nontraditional attitude filter.

The simulation results show that, in the cases of process noise bias and process noise increment, the adaptive SVD-aided UKF with multiple fading factors can adapt to changing environments better than the SaUKF. Unlike the SaUKF, which jumps over that time, the ASaUKF maintains approximately the same error level and is unaffected by process noise changes.

APPENDIX A: Proof of Theorem 2

At the first step after the bias occurring at iteration $k=\tau$ we have, the extrapolation value

$$\hat{\mathbf{x}}_b(k+1/k) = \mathbf{f}(\hat{\mathbf{x}}_b(k/k),k) = \hat{\mathbf{x}}(k+1/k) + \Delta\hat{\mathbf{x}}(k+1/k) \tag{A.1}$$

where $\Delta\hat{\mathbf{x}}(k+1/k)$ is the bias in the extrapolation value, b in the index shows that the value is biased.

Estimation value

$$\begin{aligned}\hat{\mathbf{x}}_b\left(k+1\middle|k+1\right) &= \hat{\mathbf{x}}(k+1/k)+\Delta\hat{\mathbf{x}}(k+1/k)+\mathbf{K}(k+1)\times\left[\mathbf{y}(k+1)+\mathbf{H}\boldsymbol{\delta}(k+1)-\mathbf{H}\hat{\mathbf{x}}(k+1/k)-\mathbf{H}\Delta\hat{\mathbf{x}}(k+1/k)\right]\\ &= \hat{\mathbf{x}}(k+1/k)+\mathbf{K}(k+1)\left[\mathbf{y}(k+1)-\mathbf{H}\hat{\mathbf{x}}(k+1/k)\right]+\Delta\hat{\mathbf{x}}(k+1/k)+\mathbf{K}(k+1)\mathbf{H}\boldsymbol{\delta}(k+1)-\mathbf{K}(k+1)\times\mathbf{H}\Delta\hat{\mathbf{x}}(k+1/k)\\ &= \hat{\mathbf{x}}(k+1/k+1)+\Delta\hat{\mathbf{x}}(k+1/k+1)\end{aligned}$$

(A.2)

where

$$\begin{aligned}\Delta\hat{\mathbf{x}}(k+1/k+1) &= \Delta\hat{\mathbf{x}}(k+1/k)+\mathbf{K}(k+1)\mathbf{H}\boldsymbol{\delta}(k+1)-\mathbf{K}(k+1)\mathbf{H}\Delta\hat{\mathbf{x}}(k+1/k)\\ &= \left[\mathbf{I}-\mathbf{K}(k+1)\mathbf{H}(k+1)\right]\times\Delta\hat{\mathbf{x}}(k+1/k)+\mathbf{K}(k+1)\mathbf{H}\boldsymbol{\delta}(k+1)\end{aligned} \qquad \text{(A.3)}$$

is the bias in the estimation value.

Innovation

$$\begin{aligned}\mathbf{v}_b(k+1) &= \mathbf{y}_b(k+1)-\mathbf{H}\hat{\mathbf{x}}_b(k+1/k)\\ &= \mathbf{y}(k+1)+\mathbf{H}\boldsymbol{\delta}(k+1)-\mathbf{H}\hat{\mathbf{x}}(k+1/k)-\mathbf{H}\Delta\hat{\mathbf{x}}(k+1/k)\\ &= \mathbf{v}(k+1)+\mathbf{H}\boldsymbol{\delta}(k+1)-\mathbf{H}\Delta\hat{\mathbf{x}}(k+1/k)\\ &= \mathbf{v}(k+1)+\boldsymbol{\mu}(k+1)\end{aligned} \qquad \text{(A.4)}$$

where

$$\begin{aligned}\boldsymbol{\mu}(k+1) &= \mathbf{H}\boldsymbol{\delta}(k+1)-\mathbf{H}\Delta\hat{\mathbf{x}}(k+1/k)\\ &= \mathbf{H}\left[\boldsymbol{\delta}(k+1)-\Delta\hat{\mathbf{x}}(k+1/k)\right]\end{aligned} \qquad \text{(A.5)}$$

is the innovation bias.

As seen from expression (A.5), the innovation bias is equal to the observed difference between the process bias and prediction bias. This circumstance is true for the all $k>\tau$ steps. Thus, the Theorem 2 is proved.

DATA AVAILABILITY STATEMENT:

Some or all data, models, or code that support the findings of this study are available from the corresponding author upon reasonable request.

REFERENCES:

Akhlaghi, S., N. Zhou, and Z. Huang. 2018. “Adaptive adjustment of noise covariance in Kalman filter for dynamic state estimation.” *IEEE Power and Energy Society General Meeting*, 2018-January: 1–5. IEEE Computer Society. https://doi.org/10.1109/PESGM.2017.8273755.

Almagbile, A., J. Wang, and A. Al-Rawabdeh. 2023. “An integrated adaptive Kalman filter for improving the reliability of navigation systems.” *Journal of Applied Geodesy*, 17 (3): 295–311. De Gruyter Open Ltd. https://doi.org/10.1515/JAG-2022-0048/MACHINEREADABLECITATION/RIS.

Cilden, D., H. E. Soken, and C. Hajiyev. 2017. “Nanosatellite attitude estimation from vector measurements using SVD-AIDED UKF algorithm.” *Metrology and Measurement Systems*, 24 (1): 113–125. https://doi.org/10.1515/mms-2017-0011.

Cilden-Guler, D., E. S. Conguroglu, and C. Hajiyev. 2017a. “Single-Frame Attitude Determination Methods for Nanosatellites.” *Metrology and Measurement Systems*, 24 (2): 313–324.

Cilden-Guler, D., H. E. Soken, and C. Hajiyev. 2017b. “Non-Traditional Robust UKF against Attitude Sensors Faults.” *31st International Symposium on Space Technology and Science (ISTS)*, d-077. Matsuyama-Ehime, Japan.

Gui, M., H. Yang, X. Ning, W. Ye, and C. Wei. 2023a. “A Novel Sun Direction/Solar Disk Velocity Difference Integrated Navigation Method Against Installation Error of Spectrometer Array.” *IEEE Sens J*. Institute of Electrical and Electronics Engineers Inc. https://doi.org/10.1109/JSEN.2023.3288540.

Gui, M., H. Yang, X. Ning, D. J. Zhao, L. Chen, and M. Z. Dai. 2023b. “Variational Bayesian implicit unscented Kalman filter for celestial navigation using time delay measurement.” *Advances in Space Research*, 71 (1): 756–767. Pergamon. https://doi.org/10.1016/J.ASR.2022.09.008.

Hajiyev, C., and M. Bahar. 2003. “Attitude Determination and Control System Design of the ITU-UUBF LEO1 Satellite.” *Acta Astronaut*, 52 (2–6): 493–499. https://doi.org/10.1016/S0094-5765(02)00192-3.

Hajiyev, C., D. Cilden, and Y. Somov. 2016. “Gyro-free attitude and rate estimation for a small satellite using SVD and EKF.” *Aerosp Sci Technol*, 55. https://doi.org/10.1016/j.ast.2016.06.004.

Hajiyev, C., and D. Cilden-Guler. 2017. “Review on Gyroless Attitude Determination Methods for Small Satellites.” *Progress in Aerospace Sciences*, 90: 54–66. https://doi.org/10.1016/j.paerosci.2017.03.003.

Hajiyev, C., and D. Cilden-Guler. 2023. “Attitude filtering with uncertain process and measurement noise covariance using SVD-aided adaptive UKF.” *International Journal of Robust and Nonlinear Control*, 33 (17): 10512–10531. John Wiley & Sons, Ltd. https://doi.org/10.1002/RNC.6896.

Hajiyev, C., H. E. Soken, and D. Cilden-Guler. 2019. “Nontraditional Attitude Filtering with Simultaneous Process and Measurement Covariance Adaptation.” *J Aerosp Eng*, 32 (5): 04019054. https://doi.org/10.1061/(ASCE)AS.1943-5525.0001038.

Huang, Y., Y. Zhang, P. Shi, and J. Chambers. 2021. “Variational Adaptive Kalman Filter with Gaussian-Inverse-Wishart Mixture Distribution.” *IEEE Trans Automat Contr*, 66 (4): 1786–1793. Institute of Electrical and Electronics Engineers Inc. https://doi.org/10.1109/TAC.2020.2995674.

Huang, Y., Y. Zhang, Z. Wu, N. Li, and J. Chambers. 2018. “A Novel Adaptive Kalman Filter with Inaccurate Process and Measurement Noise Covariance Matrices.” *IEEE Trans Automat Contr*, 63 (2): 594–601. Institute of Electrical and Electronics Engineers Inc. https://doi.org/10.1109/TAC.2017.2730480.

Huang, Y., F. Zhu, G. Jia, and Y. Zhang. 2020. “A Slide Window Variational Adaptive Kalman Filter.” *IEEE Transactions on Circuits and Systems II: Express Briefs*, 67 (12): 3552–3556. Institute of Electrical and Electronics Engineers Inc. https://doi.org/10.1109/TCSII.2020.2995714.

Iezzi, L., C. Petrioli, and S. Basagni. 2023. “An Adaptive Extended Kalman Filter for State and Parameter Estimation in AUV Localization.” *ICC 2023 - IEEE International Conference on Communications*, 3932–3938. IEEE. https://doi.org/10.1109/ICC45041.2023.10279557.

Julier, S. J., J. K. Uhlmann, and H. F. Durrant-Whyte. 2000. “A New Method for the Nonlinear Transformation of Means and Covariances in Filters and Estimators.” *IEEE Trans Automat Contr*, 45 (3): 477–482.

Kim, J., D. Lee, B. Kiss, and D. Kim. 2021. “An Adaptive Unscented Kalman Filter With Selective Scaling (AUKF-SS) for Overhead Cranes.” *IEEE Transactions on Industrial Electronics*, 68 (7): 6131–6140. https://doi.org/10.1109/TIE.2020.2996150.

Li, W., S. Sun, Y. Jia, and J. Du. 2016. “Robust unscented Kalman filter with adaptation of process and measurement noise covariances.” *Digit Signal Process*, 48: 93–103. Academic Press. https://doi.org/10.1016/J.DSP.2015.09.004.

Markley, F. L., and D. Mortari. 2000. “Quaternion Attitude Estimation using Vector Observations.” *Journal of the Astronautical Sciences*, 48 (2): 359–380. https://doi.org/10.1007/BF03546284.

Mimasu, B. Y., and J. C. Van der Ha. 2009. “Attitude Determination Concept for QSAT.” *Transactions of the Japan Society for Aeronautical and Space Sciences, Aerospace Technology Japan*, 7: 63–68. https://doi.org/10.2322/tstj.7.Pd_63.

Qiu, Z., Y. Huang, and H. Qian. 2020. “Adaptive robust nonlinear filtering for spacecraft attitude estimation based on additive quaternion.” *IEEE Trans Instrum Meas*, 69 (1): 100–108. Institute of Electrical and Electronics Engineers Inc. https://doi.org/10.1109/TIM.2019.2894046.

This is an Author Accepted Manuscript version.

Soken, E., and C. Hajiyev. 2011. “Adaptive Fading UKF with Q-Adaptation: Application to Pico Satellite Attitude Estimation.” *J Aerosp Eng*.

Soken, H. E., and C. Hajiyev. 2014. “Estimation of Pico Satellite Attitude Dynamics and External Torques via Unscented Kalman Filter.” *Journal of Aerospace Technology and Management*, 6 (2): 149–157. https://doi.org/10.5028/jatm.v6i2.352.

Soken, H. E., and S. ichiro Sakai. 2020. “Attitude estimation and magnetometer calibration using reconfigurable TRIAD+filtering approach.” *Aerosp Sci Technol*, 99: 105754. Elsevier Masson SAS. https://doi.org/10.1016/j.ast.2020.105754.

Springmann, J. C., and J. W. Cutler. 2014. “Flight Results of a Low-cost Attitude Determination Systems.” *Acta Astronaut*, 99: 201–214. https://doi.org/10.1016/j.actaastro.2014.02.026.

Sun, W., J. Zhao, W. Ding, and P. Sun. 2023. “Robust UKF Relative Positioning Approach for Tightly Coupled Vehicle Ad Hoc Networks Based on Adaptive M-Estimation.” *IEEE Sens J*, 23 (9): 9959–9971. Institute of Electrical and Electronics Engineers Inc. https://doi.org/10.1109/JSEN.2023.3262656.

Vinther, K., K. F. Jensen, J. A. Larsen, and R. Wisniewski. 2011. “Inexpensive Cubesat Attitude Estimation Using Quaternions And Unscented Kalman Filtering.” *Automatic Control in Aerospace*, 4 (1).

Wahba, G. 1965. “Problem 65-1: A Least Squares Estimate of Satellite Attitude.” *Society for Industrial and Applied Mathematics Review*, 7 (3): 409.

Wang, D., H. Zhang, B. Ge, C. : Wang, D. ; Zhang, and H. ; Ge. 2021. “Adaptive Unscented Kalman Filter for Target Tacking with Time-Varying Noise Covariance Based on Multi-Sensor Information Fusion.” *Sensors 2021, Vol. 21, Page 5808*, 21 (17): 5808. Multidisciplinary Digital Publishing Institute. https://doi.org/10.3390/S21175808.

Xi, Y., Z. Li, X. Zeng, X. Tang, Q. Liu, and H. Xiao. 2018. “Detection of power quality disturbances using an adaptive process noise covariance Kalman filter.” *Digit Signal Process*, 76: 34–49. Academic Press. https://doi.org/10.1016/J.DSP.2018.01.013.

Xu, T., X. Xu, D. Xu, Z. Zou, and H. Zhao. 2022. “A New Robust Filtering Method of GNSS/MINS Integrated System for Land Vehicle Navigation.” *IEEE Trans Veh Technol*, 71 (11): 11443–11453. Institute of Electrical and Electronics Engineers Inc. https://doi.org/10.1109/TVT.2022.3190298.

Xue, C., Y. Huang, C. Zhao, X. Li, L. Mihaylova, Y. Li, and J. A. Chambers. 2023. “A Gaussian-Generalized-Inverse-Gaussian Joint-Distribution-Based Adaptive MSCKF for Visual-Inertial Odometry Navigation.” *IEEE Trans Aerosp Electron Syst*, 59 (3): 2307–2328. Institute of Electrical and Electronics Engineers Inc. https://doi.org/10.1109/TAES.2022.3213787.

Zhu, F., S. Zhang, and Y. Huang. 2023. “An Adaptive Kalman Filter for SINS/GNSS Integrated Navigation with Inaccurate Process Noise Covariance Matrix Coefficient.” *2023 IEEE International Conference on Mechatronics and Automation, ICMA 2023*, 581–587. Institute of Electrical and Electronics Engineers Inc. https://doi.org/10.1109/ICMA57826.2023.10215990.

This is an Author Accepted Manuscript version.

FIGURE CAPTION LIST:

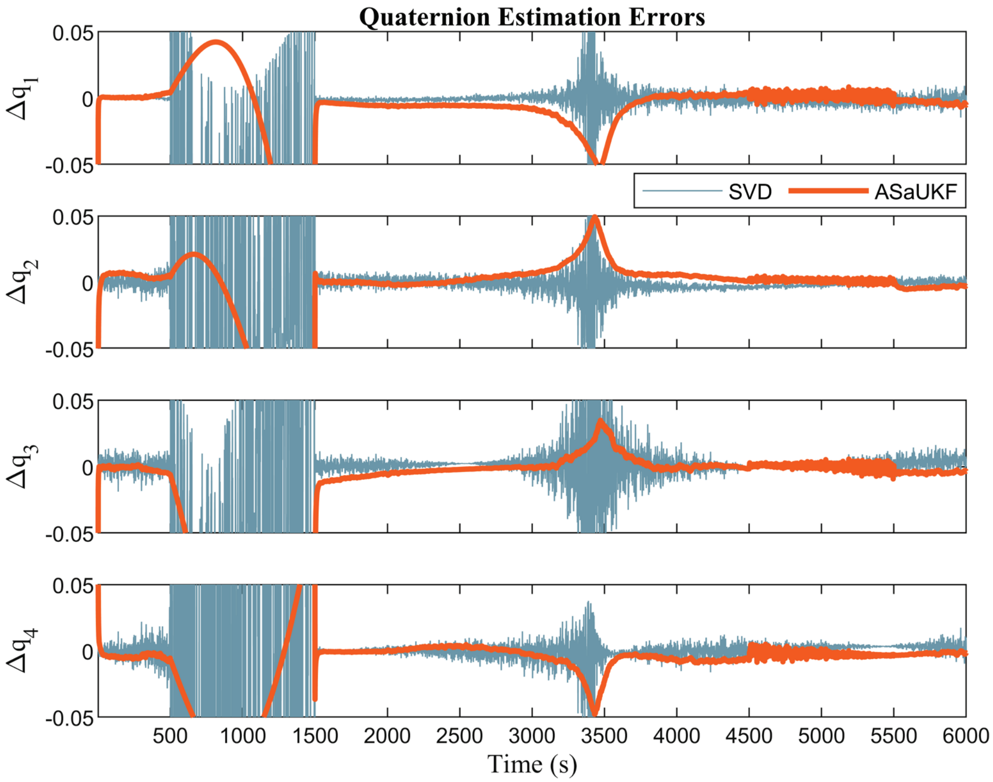

Fig. 1. ASaUKF quaternion estimation errors in the case of process noise increment η_{high}

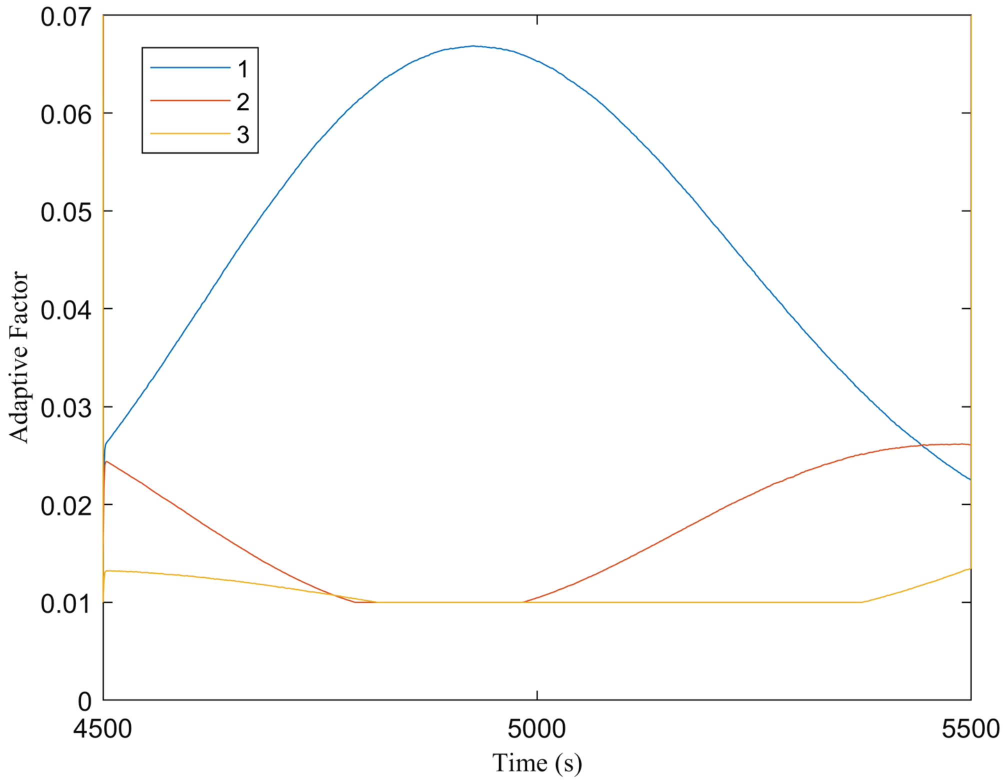

Fig. 2. ASaUKF adaptive factors in the case of process noise increment η_{high}

This is an Author Accepted Manuscript version.

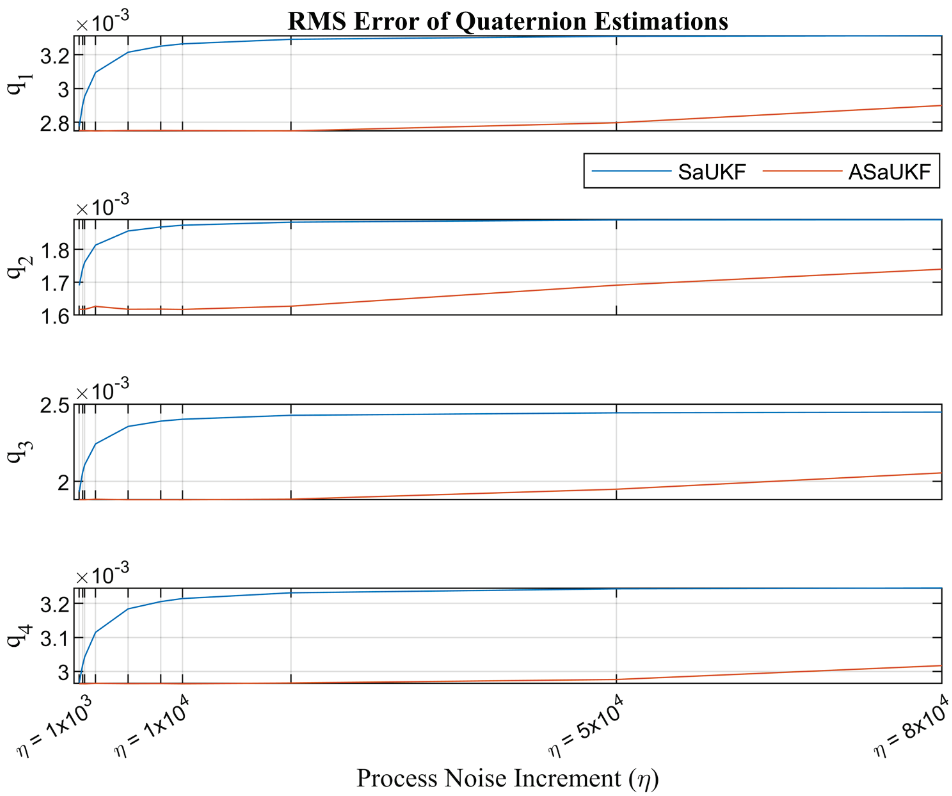

Fig. 3. SaUKF and ASaUKF RMS errors in the case of various process noise increments.

This is an Author Accepted Manuscript version.

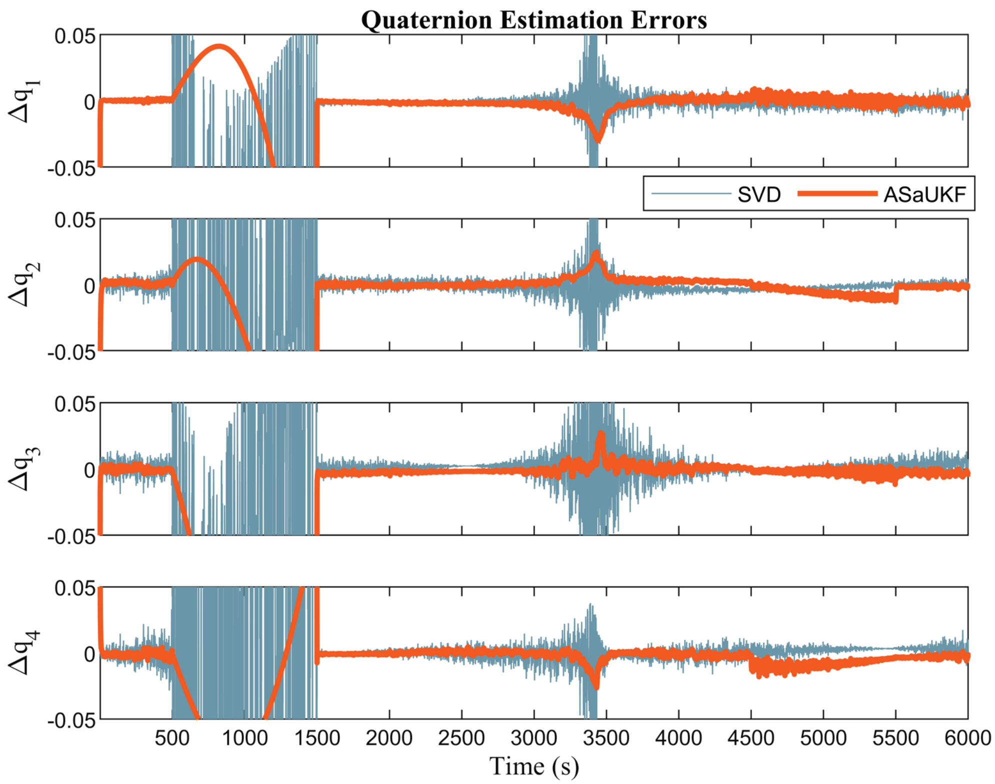

504

505 Fig. 4. ASaUKF quaternion estimation errors in the case of process noise bias δ_{high}

This is an Author Accepted Manuscript version.

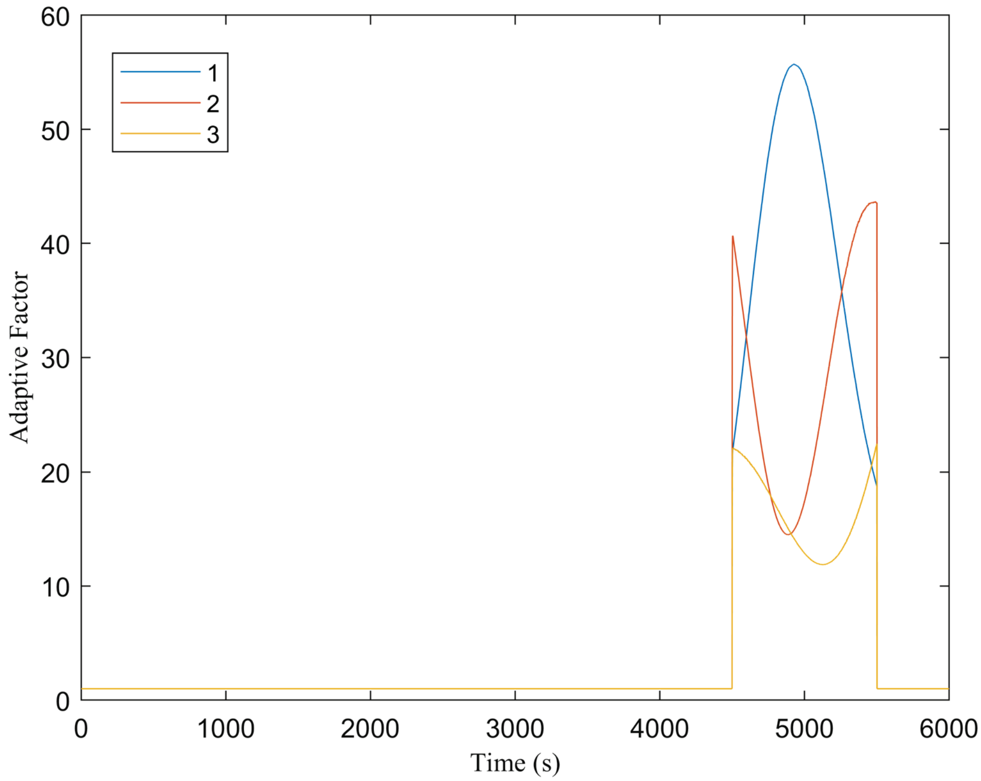

506

507 Fig. 5. ASaUKF adaptive factors in the case of process noise bias δ_{high}

508

TABLES:

Table I. Pseudocode for the implementation steps of the proposed adaptive filter.

Initial Conditions:	$\hat{\mathbf{x}}_{0\|0}, \mathbf{P}_{0\|0}$
for $k = 1{:}N$	
Prediction:	
	$\hat{\mathbf{x}}_{k\|k-1} = \mathbf{F}_k \hat{\mathbf{x}}_{k-1\|k-1}$ $\mathbf{P}^{-}{}_{k\|k-1} = \mathbf{F}_k \mathbf{P}_{k-1\|k-1} \mathbf{F}_k^{\mathrm{T}}$
Update:	
	$\mathbf{v}_k = \mathbf{y}_k - \mathbf{H}\hat{\mathbf{x}}_{k\|k-1}$ if $k \geq \tau$ $\quad \mathbf{\Lambda}_k = [\mathbf{H}^{\top}\mathbf{H}]^{-1}\mathbf{H}^{\top} \times \left[\frac{1}{M}\sum_{j=k-M+1}^{k} \mathbf{v}_j \mathbf{v}_j{}^{\top} - \mathbf{H}\mathbf{P}_{k\|k-1}\mathbf{H}^{\top} - \mathbf{R}_k\right] \times \mathbf{H}[\mathbf{Q}_k \mathbf{H}^{\top}\mathbf{H}]^{-1}$ else $\quad \mathbf{\Lambda}_k = \mathbf{I}_n$ end $\mathbf{P}^{+}{}_{k\|k-1} = \mathbf{P}^{-}{}_{k\|k-1} + \mathbf{\Lambda}_k \mathbf{Q}_k$ $\mathbf{P}_{vv_{k\|k-1}} = \mathbf{H}\mathbf{P}^{+}{}_{k\|k-1}\mathbf{H}^{\top} + \mathbf{R}_k$ $\mathbf{K}_k = \mathbf{P}^{+}{}_{k\|k-1}\mathbf{H}^{\top}\left(\mathbf{P}_{vv_{k\|k-1}}\right)^{-1}$ $\hat{\mathbf{x}}_{k\|k} = \hat{\mathbf{x}}_{k\|k-1} + \mathbf{K}_k \mathbf{v}_k$ $\mathbf{P}_{k\|k} = (\mathbf{I}_n - \mathbf{K}_k \mathbf{H})\mathbf{P}_{k\|k-1}$
end	
Outputs:	$\hat{\mathbf{x}}_{k\|k}, \mathbf{P}_{k\|k}$
Notes:	Process noise increment and/or bias occurs at the iteration step $k = \tau$. M is the width of the sliding window.

Table II. SAUKF and ASAUKF RMS errors in the case of process noise increment (averaged over 50 simulations).

RMS Error	Process Noise Increment					
	η_{low}		η_{medium}		η_{high}	
	SaUKF	ASaUKF	SaUKF	ASaUKF	SaUKF	ASaUKF
$\Delta q1$	0.00238	0.00275	0.00302	0.00274	0.00328	0.00274
$\Delta q2$	0.00170	0.00161	0.00184	0.00162	0.00188	0.00162
$\Delta q3$	0.00196	0.00188	0.00221	0.00188	0.00242	0.00188
$\Delta q4$	0.00299	0.00296	0.00308	0.00296	0.00321	0.00296
$\|\|\Delta q\|\|$	0.00461	0.00473	0.00518	0.00473	0.00551	0.00473

Table III. SAUKF and ASAUKF RMS errors in the case of process noise bias (averaged over 50 simulations).

RMS Error	Process Noise Bias					
	δ_{low}		δ_{medium}		δ_{high}	
	SaUKF	ASaUKF	SaUKF	ASaUKF	SaUKF	ASaUKF
Δq1	0.00187	0.00270	0.00198	0.00273	0.00224	0.00284
Δq2	0.00317	0.00253	0.00503	0.00429	0.00752	0.00675
Δq3	0.00193	0.00189	0.00247	0.00227	0.00325	0.00283
Δq4	0.00585	0.00509	0.00744	0.00660	0.00956	0.00869
$\|\Delta q\|$	0.00717	0.00657	0.00952	0.00863	0.01278	0.01171